International Journal of Engineering Research and Technology.
ISSN 0974-3154 Volume 11, Number 7 (2018), pp. 1085-1107

http://www.irphouse.com

Suppression of Impulse Noise in Colour Images Using Quaternion Transformation and Vector Median Filtering

Rabiu Aminu[1]
[1]*Department of Electrical Engineering, Pan African University Institute of Basic Sciences, Technology and Innovation, P.O. Box 62000—00200, Nairobi, Kenya.*

Elijah Mwangi[2]
[2]*School of Engineering, University of Nairobi, P.O. Box 30197, 00100, GPO, Nairobi, Kenya.*

Edward Ndungu[3]
[3]*Department of Telecommunication and Information Engineering, Jomo Kenyatta University of Agriculture and Technology, P.O. Box 62000—00200, Nairobi, Kenya.*

Abstract

Images are often corrupted by impulse noise due to electronic interference, switching effects, faulty charge-coupled devices, poor acquisition or recording and channel environmental degradation. This leads to the discolouration of some pixels in the image and has an adverse effect on the performance of many image application systems. In this paper, a new switching method based on the effective Quaternion transformation of colour images and vector median filtering is proposed and employed in the suppression of impulse noise. The proposed switching method comprises of two stages; impulse noise detection and image restoration. In the first stage, a Quaternion unit transform is used in detecting the corrupted pixels. In the second stage, the corrupted pixels are restored using a vector median filtering process while the noise-free ones are kept unaffected. The simulation results demonstrate that the proposed method based on the Quaternion transform achieves an acceptable balance between the details preservation and noise suppression than the classical switching filtering methods.

Keywords - Colour pixel difference, impulse noise, image restoration, noise detection, quaternion transform.

I. INTRODUCTION

Images are significant information carriers in multimedia applications such as face and finger-print detection, feature extraction, medical imaging, object detection and tracking, machine vision, remote sensing, traffic observation, surveillance systems, autonomous navigation and entertainment. However, the presence of noise reduces the quality of the image and the credibility of the information content and hence the need for restoration.

The most common types of noise found in images are additive Gaussian noise, Poisson noise, multiplicative noise and impulse noise [1], [2], [3]. Gaussian noise is mainly due to poor illumination during image acquisition, but can also be caused by imperfections in semiconductor devices. This type of noise adds certain Gaussian distribution to each pixel of the image [4]. Poisson noise is generally called photon noise and is because of variations in the number of photons sensed at a given exposure level [5]. In the multiplicative type of noise, each pixel is modulated by noise, an example of this type of noise is speckle noise. Impulse Noise (IN) is an instance where the original pixel value of an image is replaced by a signal value which is not authentic imagery. The corrupted pixels appeared as dark, bright or a white spot in the image. This type of noise is mainly due to faulty charge-coupled devices, malfunctioning of sensors during the capturing of the image, switching effects and electronic interference [6], [7]. This work focuses on the suppression of impulse noise in colour images.

The suppression of impulse noise in colour images is more challenging compared to other types of noise, because the noise value replaces the entire original pixel value. The corrupted pixels appeared significantly different from their neighbours. Thus, the Quaternion distance measure is employed in this work to take advantage of these dissimilarities to detect the pixels contaminated by impulse noise.

Over the years, several non-linear vector filters have been developed for removal of impulse noise in colour images such as [2], [8], [9], [10]. Among these class of filters, the most widely used is Vector Median Filter (VMF) which employed the measure of the dissimilarity between colour pixels. Euclidean and Manhattan distances are the most common measures employed in these class of filters [11]. However, other distance measures can be employed to detect and suppress impulse noise. The major weaknesses of vector median filters are image blurring and reduction in edge sharpness. To address these problems, the Weighted Vector Median Filter was introduced [12]. However, this filter also causes loss of image details, because both the contaminated pixels and noise-free pixels are modified by the filter. This has led to the search of new techniques that do not have such adverse effects.

The most widely used of these new techniques are the two stage detection/restoration methods. The first stage involves the detection of the corrupted pixels and the second stage the suppression of impulse noise. The two stage detection/restoration method also known as switching strategy provides adequate solution to image detail loss. In

the past few years, many techniques based on switching strategy have been proposed for impulse noise removal in colour images such as [13], [14], [15]. Other filters developed based on switching strategy are the Trimmed Adaptive Switching Bilateral Filter (TASBF) [7], Adaptive Centre Weighted Vector Median Filter (ACWVMF) [12], Adaptive Marginal Median Filter (AMMF) [16], Adaptive Rank Weighted Switching Filter (ARWSF) [17], Fast Averaging Peer Group Filter (FAPGF) [18] and an Efficient Weighted-Average Filter (EWAF) [19]. To improve the efficiency of impulse noise suppression, other techniques have been introduced recently.

In [20] and [21], A new detection statistic for random-valued impulse noise removal in colour images was proposed. This method is based on a new statistic called Rank-Ordered Logarithmic Difference, ROLD for short which is an improvement of Rank Ordered Absolute Difference (ROAD). It uses a logarithmic function to increase ROAD values while keeping the small ROAD values from any significant change. This method provides more accurate noise detection, because of its ability to distinguish noise values of neighbouring pixels that are close to each other. The major weakness of this technique is that the noise detection capability relies wholly on the parameters that control the shape of the logarithmic function. For this reason, the selection of these parameters is challenging.

A fuzzy two-step colour filter was introduced in [22] . The method used gradient values to group colour pixels into noisy and noise-free ones. The corrupted pixels are filtered by an iterative fuzzy filtering technique while the noise-free ones are unchanged. However, this method treats the three colour components separately in the detection stage [23].

Histogram-based fuzzy colour filter for image restoration was proposed in [24] and [25]. The filter uses colour component differences to detect pixels that are contaminated by impulse noise. It has three stages: the approximation of the original histogram of the colour channels differences, the construction of appropriate fuzzy sets for representing the linguistic values of these differences and the construction of fuzzy rules that define the filter output [24].

To enhance the noise detection accuracy and image details preservation, switching methods based on the Quaternion theory are presented in [3], [11], [26], [27] and [28]. These filters used Quaternion distance measure to detect the contaminated pixels before employing a suitable filtering method to remove the noise in the contaminated pixels. In [27], only the chromaticity component is considered in detecting the noisy pixels. The major limitation of this method is that it cannot distinguish pixels that are achromatic from their neighbours. Especially pixels on the gray line with colour components $R=G=B$. In conclusion, these filters achieve acceptable filtering results for colour images corrupted by impulse noise and prove that quaternion distance measure is effective for impulse noise detection. However, the noise detection accuracy of these filters reduce sharply with the increases in the noise density.

This paper proposes a switching method based on the effective Quaternion transformation of colour images and vector median filtering. The chromaticity, intensity and saturation differences are employed in detecting the impulse noise. A vector median filtering process is employed to suppress the noise in the contaminated pixels without modifying the entire image.

The rest of this paper is organized as follows: Impulse noise models and performance measures are introduced in section II. The properties of Quaternion and its applications in colour images are discussed in section III. The proposed filter based on the Quaternion transformation and vector median filtering is presented in section IV. Simulation results and analysis are given in section V. Finally, a conclusion is given in section VI.

II. IMPULSE NOISE MODELS AND PERFORMANCE MEASURES

The common types of impulse noise found in colour images can be generally classified into: fixed value also known as Salt and Pepper (S&P) and Random-Valued impulse (RVI) noise models. These two impulse noise models are expressed in (1) and (2).

$$C_Q(x,y) = \begin{cases} 0 \text{ or } 255 & : \textit{with probability } p \\ f(x,y) & : \textit{with probability } 1 - p \end{cases} \quad (1)$$

$$C_Q(x,y) = \begin{cases} \eta(\mathrm{x,y}) & : \textit{with probability } p \\ f(x,y) & : \textit{with probability } 1 - p \end{cases} \quad (2)$$

Where (x, y) represents the spatial coordinates of the image, $C_Q(x, y)$ is the corrupted image, *f (x, y)* represents the noise-free image and $\eta(x, y)$ denotes the noise, *p* is the corruption probability defined in the range of 0 to 1 and *Q* denotes the three colour channels. For S&P noise model, the value of the corrupted pixels is either 0 or 255 for an 8-bit image. In the RVI noise model, the value of the contaminated pixels is uniformly distributed in the range of 0 to 255 for an 8-bit image.

Three objective and one subjective measures are employed to evaluate the performance of the developed algorithm. The objective measures are: Peak Signal-to-Noise Ratio (PSNR), Mean Absolute Error (MAE) and Structural Similarity Index (SSIM). The PSNR, MAE and SSIM are mathematical tools used to measure the differences between the original image and the image processed by the proposed method. The MAE and PSNR are defined in (3) and (4) while SSIM is defined in [29].

The subjective measure is based on visual assessment of the original image and the image processed by the developed method.

$$MAE = \frac{\sum_{Q=1}^{3}\sum_{x=1}^{M}\sum_{y=1}^{N}\left| f(x,y) - \overline{f}(x,y)\right|}{3MN} \qquad (3)$$

$$PSNR = 20\log\frac{255}{\sqrt{\frac{\sum_{Q=1}^{3}\sum_{x=1}^{M}\sum_{y=1}^{N}\left[f(x,y) - \overline{f}(x,y)\right]^2}{3MN}}} \qquad (4)$$

Where $f(x,y)$ is the original colour image, $\overline{f}(x,y)$ the filtered colour image of dimension $M \times N$ and Q is the three colour channels.

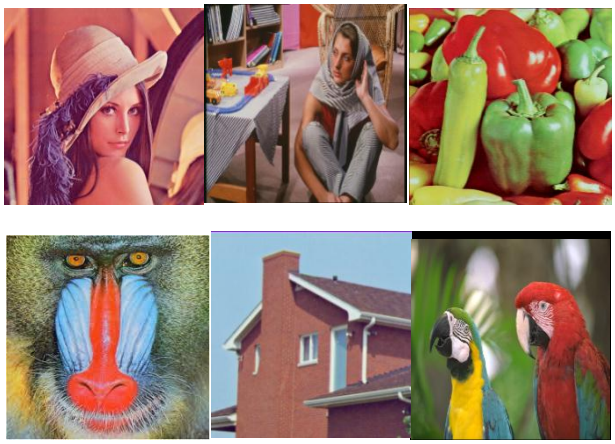

Fig. 1: The test image set: *Lena, Barbara, Peppers, Mandrill, House and Parrots*

III. THE PROPERTIES OF QUATERNIONS AND ITS APPLICATIONS IN COLOUR IMAGES

III.I. Properties of Quaternions

The Quaternion is an expansion of a conventional two dimensional complex number (2D) to a four dimensional complex number (4D) [11], [26], [27]. A Quaternion number q has three imaginary parts and one real part and is usually expressed in complex form as:

$$q = a + bi + cj + dk \qquad (5)$$

Where $a, b, c, d \in \mathbb{R}$ and i, j, and k are complex operators. These complex operators fulfill the following rules:

$$i^2 = j^2 = k^2 = ijk = -1$$

$$ij = k, \quad jk = i, \; ki = j$$

$$ji = -k, \; kj = -i, \; ik = -j$$

$$\text{Also, } i(jk) = (ij)k \qquad (6)$$

Therefore, multiplication operation between Quaternions is not commutative but associative. A pure Quaternion has the real part value equal to zero as expressed in equation (7)

$$q_{pure} = bi + cj + dk \qquad (7)$$

Other properties of Quaternion are the complex conjugate and modulus as expressed in equation (8) and (9).

$$\bar{q} = a - bi - cj - dk \qquad (8)$$

$$|q| = \sqrt{q\bar{q}} = \sqrt{a^2 + b^2 + c^2 + d^2} \qquad (9)$$

In polar form, the Quaternion is given by:

$$q = |q|e^{\mu\theta} = |q|[\cos\theta + \mu\sin\theta] \qquad (10)$$

Dividing a non-zero Quaternion q by its modulus produces a term called the unit Quaternion. A unit pure Quaternion is obtained by dividing a non-zero pure quaternion by its modulus as expressed in (11).

$$\mu = \frac{1}{\sqrt{3}}(i + j + k) \qquad (11)$$

III.II. Quaternion Representation of Colour Images

A standard *RGB* colour image consists of three colour components: the Red, Green and Blue. Similarly, a pure Quaternion consists of three imaginary parts. Thus, an *RGB* colour image can be expressed in terms of pure Quaternion as given in (12).

$$q(x, y) = R(x, y)i + G(x, y)j + B(x, y)k \qquad (12)$$

Note: x, y are the coordinates of the colour pixel and R, G, $B \in [0,1,2.....255]$ denote the intensity values of the pixel in the three colour components for an 8-bit image. Thus, a whole three dimensional *RGB* colour pixel can be represented as one pure Quaternion number. To analytically express a colour image using Quaternion, a Quaternion unit vector U is defined as follows:

$$U = \cos\theta + \mu\sin\theta \qquad (13)$$

Where μ is the unit pure Quaternion defined in (11). In the *RGB* domain, μ represents a gray-line, where a colour pixel is achromatic and the three colour components have the same magnitude.

III.III. The Quaternion Unit Transform and Colour Pixel Difference

In the *RGB* format the Quaternion unit transform of a colour pixel is given by:

$$\begin{aligned} Y &= Uq\overline{U} \\ &= (\cos\theta + \mu\sin\theta)q(\cos\theta - \mu\sin\theta) \\ &= q\cos 2\theta + 2\mu[\mu.q]\sin^2\theta + \mu \times q\sin 2\theta \\ &= (Ri + Gj + Bk)\cos 2\theta + \frac{2}{\sqrt{3}}\mu(R+G+B)\sin^2\theta \\ &+ \frac{1}{\sqrt{3}}[(B-G)i + (R-B)j + (G-R)k]\sin 2\theta \\ &= Y_{RGB} + Y_I + Y_C \end{aligned} \qquad (14)$$

Where;

q is given in equation (12)

$$Y_{RGB} = (Ri + Gj + Bk)\cos 2\theta$$

$$Y_I = \frac{2}{\sqrt{3}}\mu(R+G+B)\sin^2\theta \text{ and}$$

$Y_C = \frac{1}{\sqrt{3}}[(B-G)i + (R-B)j + (G-R)k]\sin 2\theta$ Y_{RGB} represents the *RGB* colour space, Y_I is the intensity of the colour pixel and Y_C denotes the colour difference also known as chromaticity of a colour pixel. Assume that: $\theta = \frac{\pi}{4}$,

$T = U\Big|_{\theta=\frac{\pi}{4}} = \frac{1}{\sqrt{2}} + \frac{1}{\sqrt{6}}(i+j+k)$ and denote $G_0 = Tq\overline{T}$ then $Y_{RGB} = 0$,

$Y_I = \frac{1}{3}[(R+G+B)(i+j+k)]$ and $Y_C = \frac{1}{\sqrt{3}}[(B-G)i + (R-B)j + (G-R)k]$.

Likewise, $\overline{G}_0$ can be expressed as follows:

$$\begin{aligned} \overline{G}_0 &= \overline{T}qT = \frac{1}{3}[(R+G+B)(i+j+k)] \\ &- \frac{1}{\sqrt{3}}[(B-G)i + (R-B)j + (G-R)k] \end{aligned} \qquad (15)$$

Thus:

$$Y_I = \frac{1}{2}(G_0 + \overline{G}_0) \qquad (16)$$

$$Y_C = \frac{1}{2}(G_0 - \overline{G}_0) \qquad (17)$$

Suppose two colour pixels are given by q_1 and q_2, their intensity and chromaticity differences can be defined as follows:

$$d_1(q_1, q_2) = \frac{1}{2}\left|\left(G_{o1} + \bar{G}_{o1}\right) - \left(G_{o2} + \bar{G}_{o2}\right)\right| \qquad (18)$$

$$d_2(q_1, q_2) = \frac{1}{2}\left|\left(G_{o1} - \bar{G}_{o1}\right) - \left(G_{o2} - \bar{G}_{o2}\right)\right| \qquad (19)$$

To ensure the uniqueness and efficiency of the proposed Quaternion distance measure, a saturation difference between two colour pixels is defined and added to both chromaticity difference and intensity difference. In HSI (Hue, Saturation, Intensity) colour space, the saturation (colour purity) of a colour pixel is defined as

$$Y_S = 1 - \frac{3}{(R+G+B)}[min(R,G,B)] \qquad (20)$$

Given two colour pixels q_1 and q_2, their saturation difference can be computed as $d_3(q_1, q_2) = Y_{S1} - Y_{S2}$. Therefore, in this paper the chromaticity, the intensity and the saturation differences of colour pixel are considered to determine whether a colour pixel is noisy or a noise-free one. Zhu et.al [28] employed the multiplication operator to combine the brightness distance and the chromaticity distance to detect a noisy pixel in a colour image. Similarly, the same operator is employed in this paper to combine the chromaticity difference, the intensity difference and the saturation difference and then the distance between two colour pixels can be expressed as:

$$d(q_1, q_2) = \left[d_1(q_1, q_2) + d_3(q_1, q_2)\right]^{\gamma} + \left[d_2(q_1, q_2) + d_3(q_1, q_2)\right]^{\gamma - 1} \qquad (21)$$

Equation (21) sums the chromaticity, the intensity and the saturation differences of colour pixels, which is referred as Quaternion distance measure. The parameter γ controls the chromaticity difference and the intensity difference. In [28], γ was set to 0.75, the same value γ=0.75 is also use in this paper. Smaller or larger value of γ will change $d(q_1, q_2)$ significantly and result in pixel misclassification.

IV. THE PROPOSED QUATERNION SWITCHING MEDIAN FILTER

The first and most important stage in any noise removal algorithm is detection process. The objective of noise detection is to determine whether a pixel is noisy or pure. The proposed Switching Median Filter (QSMF) based on the Quaternion unit transform theory is presented in this section. The QSMF employs Quaternion distance

measure in the noise detection process. If a colour pixel is detected as noisy, then a Vector Median Filtering (VMF) process will be used to replace it otherwise it remains unchanged. As shown in Fig. 2, the proposed method first converts a contaminated colour image from the *RGB* (Red, Green and Blue) colour space into the Quaternion format. It then computes the colour difference between the pixels before classifying them into noisy and noise-free ones. After calculating the Quaternion distances between a pixel and its eight neighbours, the result is compared to a predetermined threshold T_h to conclude if a pixel is corrupted by a noise or is a good one. The vector median filtering process is used to replace a noisy pixel.

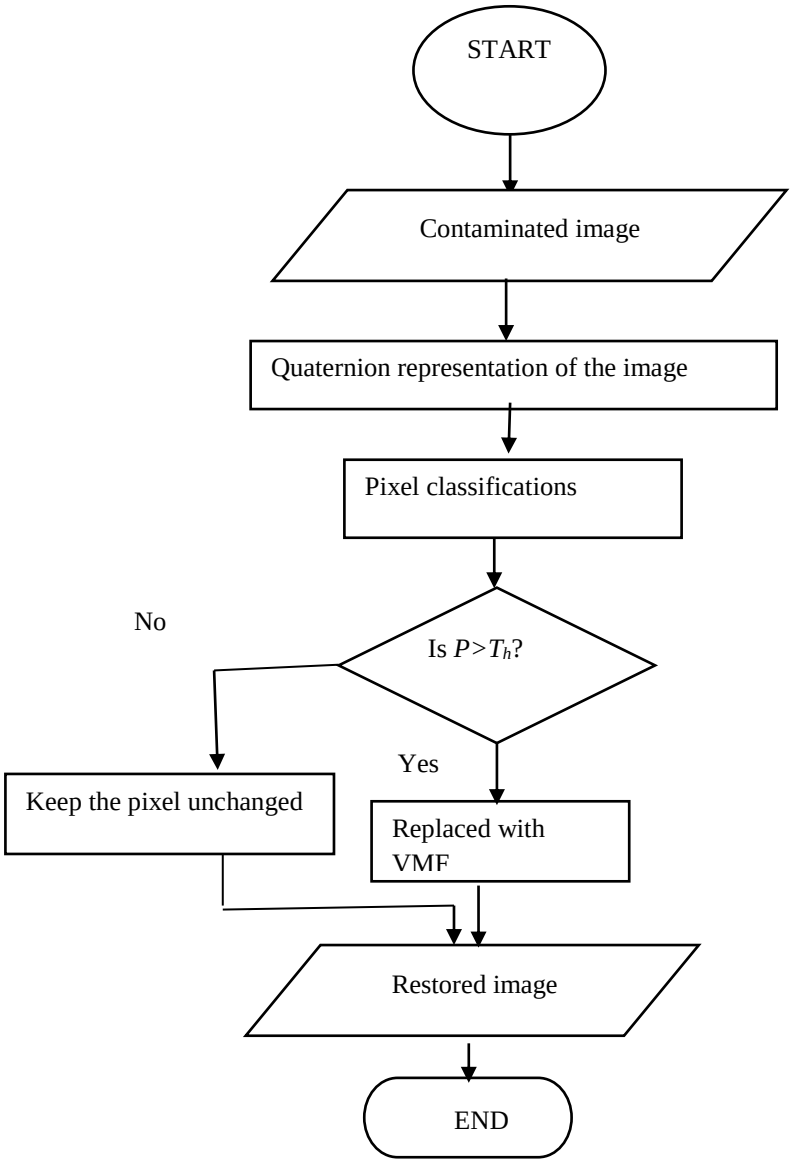

Fig. 2: Flowchart of the proposed switching filtering method

Consider a filtering window of size 3×3 denoted by:

$$\begin{pmatrix} q_1 & q_2 & q_3 \\ q_4 & q_5 & q_6 \\ q_7 & q_8 & q_9 \end{pmatrix}$$

The Quaternion distance between the filtering window center pixel q_5 and its eight neighbouring pixels in the directions of 0^0, 45^0, 90^0 and 135^0 can be expressed as follows:

$$P_{0^0} = \frac{1}{2}\left[d(q_4, q_5) + d(q_5, q_6)\right] \qquad (22)$$

$$P_{45^0} = \frac{1}{2}\left[d(q_3, q_5) + d(q_5, q_7)\right] \qquad (23)$$

$$P_{90^0} = \frac{1}{2}\left[d(q_2, q_5) + d(q_5, q_8)\right] \qquad (24)$$

$$P_{135^0} = \frac{1}{2}\left[d(q_1, q_5) + d(q_5, q_9)\right] \qquad (25)$$

From equation (22) - (25), it can be observed that if q_5 belongs to the edge of an image, then at least one of the $Pj\ (j=0^0, 45^0, 90^0, 135^0)$ will be extremely small. On the other hand, when q_5 belongs to the smooth area of an image $Pj\ (j=0^0, 45^0, 90^0, 135^0)$ will all be zero. When q_5 is contaminated by impulse noise, all the values $Pj\ (j=0^0, 45^0, 90^0, 135^0)$ will turn significantly bigger than zero irrespective of where the pixel is positioned in the image. To efficiently detect the contaminated pixels and noise-free ones, a predetermined threshold T_h is set. If $P=min\{Pj, (j=0^0, 45^0, 90^0, 135^0)\}$ is greater than T_h, the filtering window operating pixel is concluded as noisy. Otherwise the filtering window operating pixel is concluded as noise-free.

The second stage of the proposed method is the suppression of the impulse noise in the contaminated pixels. In the proposed method, a vector median filtering process is employed for this purpose. The vector median filter (VMF) in Quaternion form is defined as:

$$q_{(x,y)}^{VMF} = \underset{q_i \in \{q_1, q_2, q_3 \ldots\ldots q_N\}}{argmin} \sum_{j=1}^{N} \left\| q_j - q_i \right\| \qquad (26)$$

Where x, y represent the operating pixel position in the image, j and i indicate the rows and the columns where the pixels belong in the filtering window. $N = 3 \times 3$ is the set of pixels contain in the filtering window and $[q_1, q_2, q_3 \ldots\ldots q_N]$ denotes all the pixels in Quaternion form in the filtering window.

From the above deduction, the QSMF can be implemented as follows:

$$q_{(x,y)}^{QSMF} = \begin{cases} q_{(x,y)}^{VMF} & If \quad P > T_h, \\ q_{(x,y)} & otherwise \end{cases} \qquad (27)$$

A filtering window W of size 3×3 is used in this paper, the neighbours of the operating pixel (q_5) may be contaminated with impulse noise, especially if the noise density is very high. To ensure the corrupted pixels are detected effectively, some of the neighbours of $q5$ come from filtered results. For example, when filtering the colour pixel (q_5), the pixels q_1, q_2, q_3 and q_4 should come from filtered results while q_5, q_6, q_7, q_8 and q_9 take their original values.

V. SIMULATION RESULTS AND ANALYSIS

This section provides several experiments and comparison results to assess the performance of the developed QSMF. For all the experiments, the 8-bit standard colour test images *Lena (Len), Barbara (Bar), Peppers (Pep), Mandrill (Man), House (Hou)* and *Parrots (Par)* depicted in Fig.1 were used.

V.I. Optimal Threshold Selection

The threshold T_h is an important factor in the proposed algorithm. Thus, experiments are performed to obtain the optimum value of T_h. The dependence of the PSNR on the threshold T_h for the six selected test images corrupted with different levels of S&P and RVI noise models is depicted in Fig. 3, 4, 5, 6, 7 and 8. It can be observed that as T_h gets closer to 0, the QSMF becomes the conventional VMF and achieves a superior noise suppression capability. Then again, as T_h value turns larger, the QSMF becomes an identity filter and performed no filtering operation.

Fig. 3, 4 and 5 shows the simulation results obtained when filtering the six test images corrupted by 5%, 15% and 30% S&P noise model. It can be observed that the optimal threshold is diverse for each image and impulse noise contamination level.

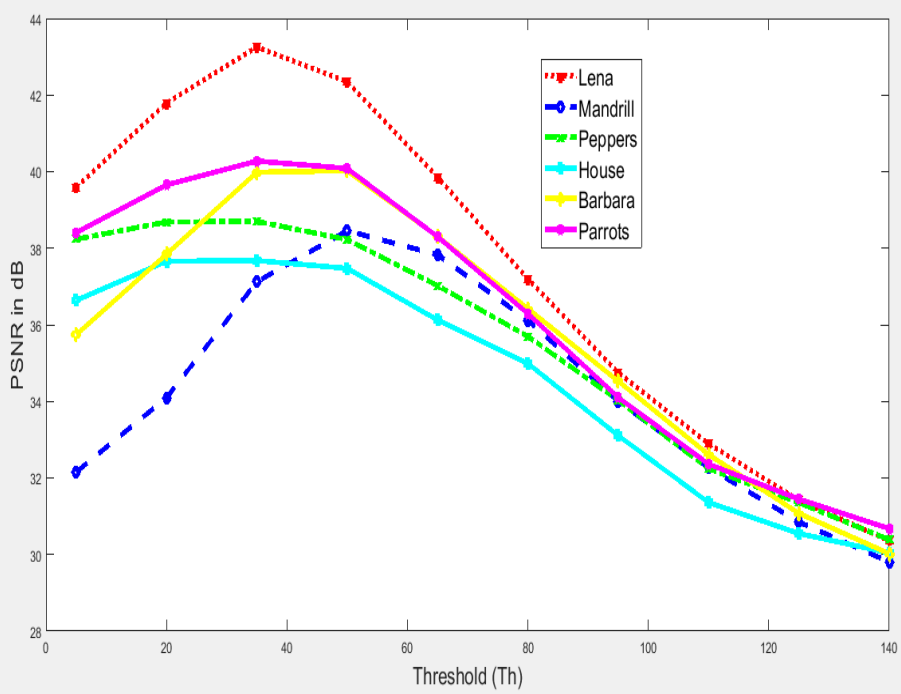

Fig. 3: Test image set contaminateted by 5% S&P noise model

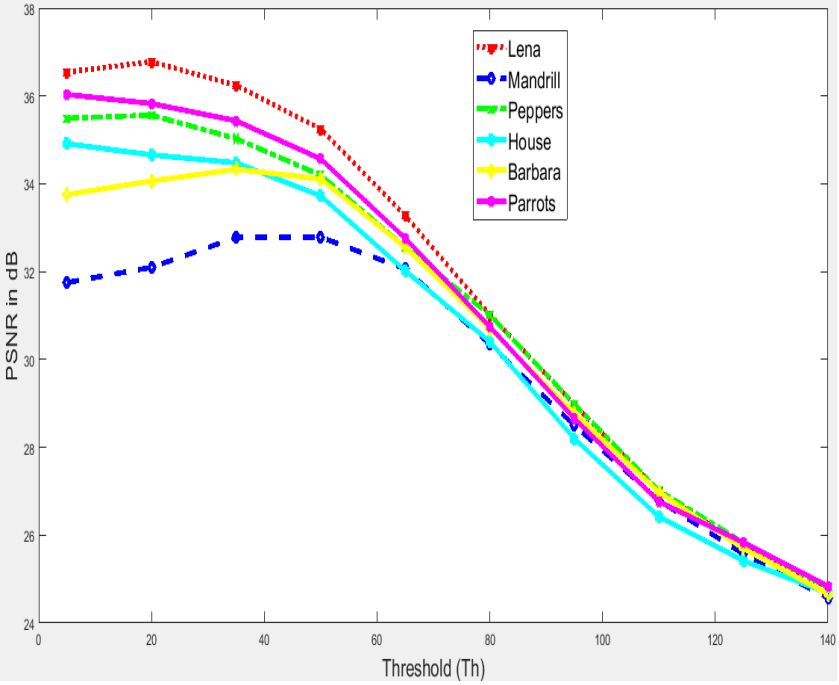

Fig. 4: Test image set contaminated by 15% S&P noise model

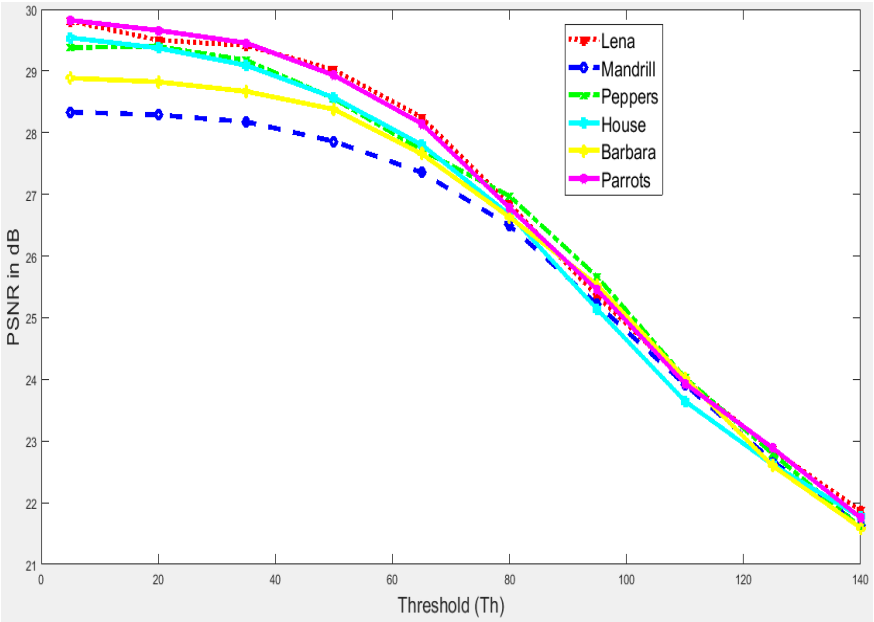

Fig. 5: Test image set contaminated by 30% S&P noise model

Fig. 6, 7 and 8 shows the simulation results obtained when filtering the six test images contaminated with 5%, 15% and 30% RVI noise model. The results show that the optimal threshold is diverse for each image and noise contamination level. Smaller value of T_h achieves better PSNR results when the noise density is high. Whereas, T_h has to be large to achieve a good results when the noise density is low.

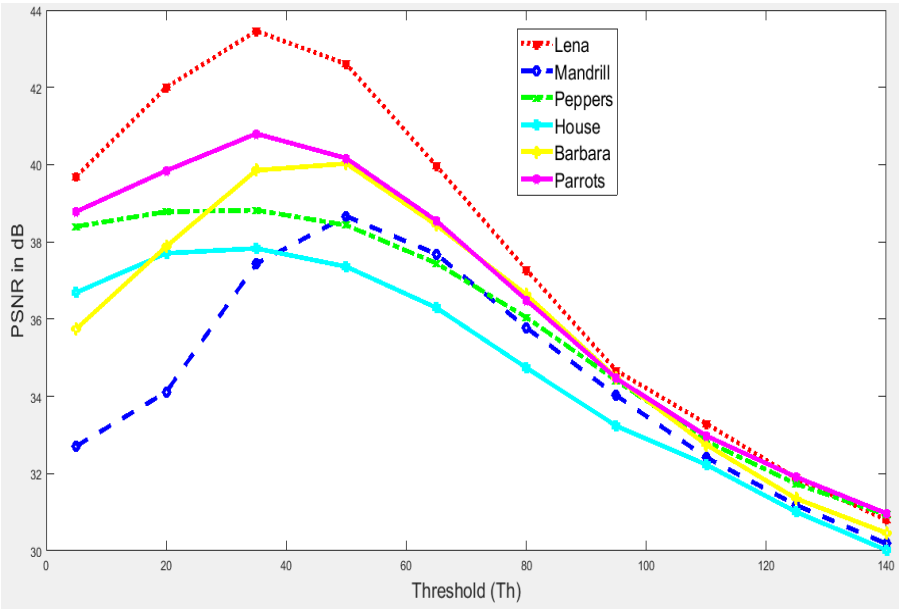

Fig. 6: Test image set contaminated by 5% RVI noise model

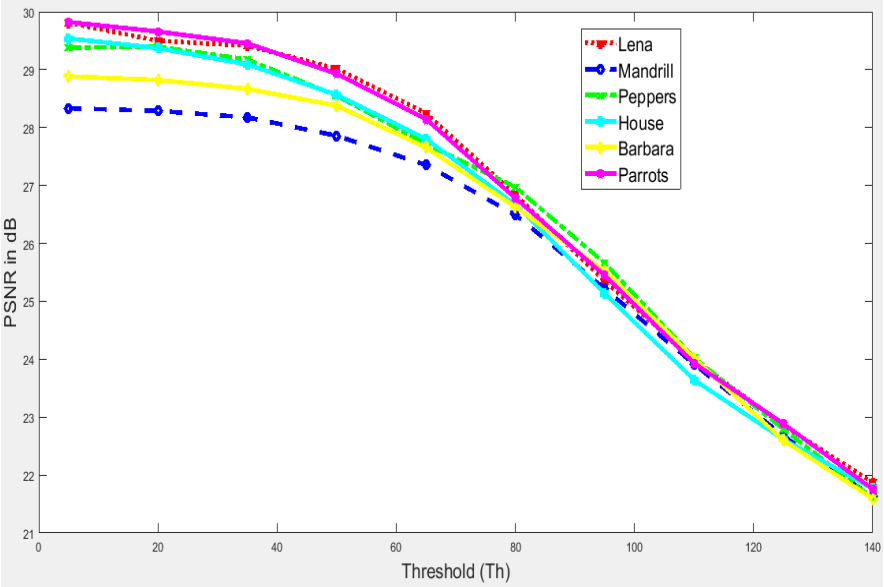

Fig. 7: Test image set contaminated by 15% RVI noise model

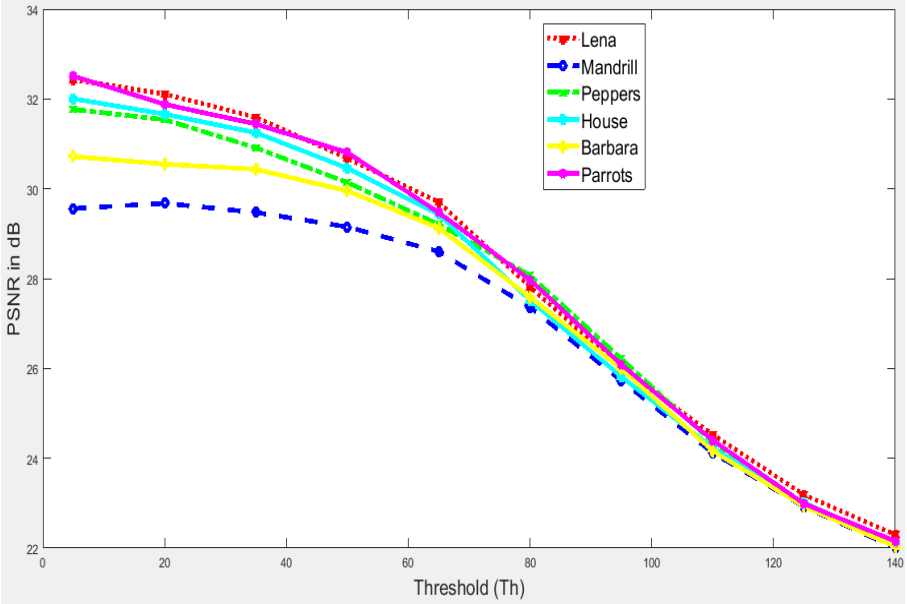

Fig. 8: Test image set contaminated by 30% RVI noise model

It can be observed from Fig. 3 to 8 that the largest value of PSNR is achieved by setting $T_h=35$, when filtering the colour *Lena* image contaminated by 5% RVI noise model. However, this value is not the same when filtering the other five test images. In general, T_h varies with the image type, impulse noise model and the noise density. The idea is to choose the optimal value that will give the best performance in all

cases. A best experimental results can be obtained by using $T_h=40$ in everyone of the cases. Therefore, this value of T_h is utilized for the remaining experiments in this paper.

V.II. Evaluation of the Noise Detection Accuracy of the Proposed QSMF

Noise detection is considered to be the most important stage in a switching filter, hence, it is very essential to assess the performance of the noise detection capability of the developed filter first. In [11] and [26], the accuracy rate (ε_1), the detection rate (ε_2) and the false detection rate (FDR) were employed to asses the noise detection capability of the work. Similarly, the same parametes are employed to asses the noise detection capabilty of the proposed QSMF. The result is presented in Table I.

In the experiment, the test image set corrupted by 5%, 15% and 30% noise contamination probability of the S&P and RVI noise models are considered for evaluating the noise detection ability of the proposed filter. It can be observed from Table I that both ε_1 and ε_2 are greater than 0.7 for S&P noise model and the maximum value of FDR is 28.9%. This shows that the noise detection algorithm is very effective. For an image corrupted by RVI noise, the effectiveness level is less than that of S&P because the detection of the noisy pixels is more challenging due to the fact that in RVI noise model there are minor dissimilarities between the noisy pixels and their neighbours.

Another reason is that, the RVI noise model is not correlated as such the channel noise contamination probability is less than the noise contamination probability. Another important point to note is that, the noise detection efficiency is higher in the images with natural features (*Lena, Mandrill, Barbara, Peppers and Parrots*). Whereas, the effeciency reduced significantly in the images with man-made features such as *House*. This could be due to the limitation of the Quaternion distance measure in distinguishing the achromatic nature of the colour pixels in the man-made images.

In the next experiment, the 256×256 8-bit colour *Lena* and *Mandrill* test images conterminated with 5%, 10%, 15%, 20%, 25%, 30%, 35% and 40% for SNP and RVI noise model have been filtered using the proposed method. The objective measures result is shown in Table II and III.

Table I: Experimental Result of Noise Detection Capability Using Six Test Images Corrupted With 5%, 15% and 30% Noise Density for S&P and RVI Impulse Noise Models

Test image	S&P			RVI		
	ε_1	ε_2	FDR (%)	ε_1	ε_2	FDR (%)
Lena 5%	0.879	0.850	25.6	0.847	0.843	41.9
Lena 15%	0.853	0.849	22.0	0.841	0.839	31.4
Lena 30%	0.839	0.845	18.5	0.833	0.826	23.5
Mandrill 5%	0.856	0.890	26.2	0.856	0.840	39.2
Mandrill 15%	0.857	0.856	18.8	0.847	0.842	29.6
Mandrill 30%	0.828	0.834	17.5	0.850	0.840	22.4
House 5%	0.767	0.800	26.7	0.770	0.748	45.9
House 15%	0.745	0.744	20.0	0.736	0.745	34.4
House 30%	0.728	0.740	17.6	0.731	0.730	25.2
Peppers 5%	0.897	0.891	28.9	0.875	0.890	36.6
Peppers 15%	0.886	0.883	21.9	0.877	0.868	27.9
Peppers 30%	0.867	0.88	19.5	0.849	0.857	21.3
Barbara 5%	0.895	0.881	28.6	0.870	0.892	36.1
Barbara 15%	0.871	0.860	20.5	0.855	0.870	27.6
Barbara 30%	0.855	0.864	18.5	0.849	0.839	21.2
Parrots 5%	0.840	0.870	27.9	0.823	0.850	34.1
Parrots 15%	0.819	0.815	21.3	0.817	0.809	26.2
Parrots 30%	0.799	0.794	19.3	0.820	0.805	20.4

It can be seen that the performance of the QSMF depends mainly on noise density, test image and noise model used. Table II and III shows that the efficiency of the proposed filter decreases with increase in the noise density as expected. It is also shown that the efficiency of the proposed method reduced when filtering the colour

House image because of the achromatic nature of the pixels in the image. In summary, the results shows that the performance of the developed filter is proved effective in all cases.

Table II: MAE, MSE and PSNR Results When Filtering the Colour *Lena* Image Corrupted With 5%-40% with an Interval of 5% for S&P and RVI Noise Models

Noise Level	S&P noise model			RVI noise model		
	MAE	SSIM	PSNR (dB)	MAE	SSIM	PSNR (dB)
5%	0.156	0.976	43.3	0.156	0.980	42.2
10%	0.315	0.962	39.4	0.309	0.966	39.7
15%	0.516	0.938	36.1	0.485	0.952	37.1
20%	0.728	0.915	33.8	0.665	0.931	35.2
25%	0.978	0.888	31.6	0.879	0.906	33.3
30%	1.336	0.852	29.1	1.106	0.882	31.5
35%	1.797	0.800	27.5	1.409	0.844	29.7
40%	2.257	0.755	25.5	1.818	0.803	27.9

Table III: MAE, MSE and PSNR Results When Filtering the Colour *Mandrill* Image Corrupted With 5%-40% with an Interval of 5% for S&P and RVI Noise Models

Noise Level	S&P noise model			RVI noise model		
	MAE	SSIM	PSNR (dB)	MAE	SSIM	PSNR (dB)
5%	0.431	0.901	37.9	0.423	0.962	37.9
10%	0.804	0.888	35.1	0.774	0.938	35.1
15%	1.198	0.871	33.1	1.133	0.918	33.4
20%	1.595	0.856	31.1	1.486	0.890	32.0
25%	1.991	0.828	29.6	1.852	0.865	30.5
30%	2.392	0.798	28.1	2.183	0.836	29.4
35%	2.863	0.766	26.5	2.541	0.806	28.2
40%	3.446	0.733	25.0	2.952	0.777	26.9

V.III. Performance Comparison

In this section, the QSMF is compared to the traditional Vector Median Filter (VMF) and other classical developed switching filters. The filters selected for the comparison are the Identity Filter (IF) [11], the traditional VMF [11], the Adaptive Rank Weighted Switching Filter (RSAWF) [17], the Fast Averaging Peer Group Filter (FAPGF) [18], the Fuzzy Two-Step Colour Filter (FTSCF) [22], the Histogram-Based Fuzzy Colour filter (HFC) [24], the Quaternion-based Colour Difference Measure Filter (QCDMF) [27], the Quaternion Switching Vector Median Filter Based on Local Reachability Density [28] shorten as QSVMF-CLRD and the impulse noise removal from colour imges using fusion technique (FTF) [30]. The results are shown in Table IV and V.

Table IV: Comparison Results in PSNR (dB) When Filtering the 512×512 Colour *Lena* Image Corrupted With 10%, 20% and 30% of S&P Noise Model

Filter	Noise density		
	10%	20%	30%
Noisy_image	15.27	12.25	10.48
VMF	30.04	26.81	22.56
RSAWF	38.89	35.58	32.76
QCDMF	55.93	54.85	41.12
FTSCF	51.40	45.70	38.60
HFC	51.50	46.80	41.40
QSMF (proposed)	**56.78**	**53.95**	**42.01**

Table V: Comparison in PSNR dB When Filtering the 256×256 *Parrots* Colour Image Corrupted With 10%, 20% and 30% of RVI Noise Model

Filter	Noise density		
	10%	20%	30%
Noisy_image	16.51	13.47	11.73
VMF	31.33	28.56	24.53
FAPGF	36.47	35.69	33.93
QSVMF-CLRD	38.69	31.62	29.68
FTF	38.56	36.86	35.47
QSMF (proposed)	**39.27**	**37.81**	**35.95**

The filtering results presented in Tables IV and V show the comparison in terms of the objective measures using *Lena* and *Parrots* test image corrupted with S&P and RVI noise models at 10%, 20% and 30% noise density. After analyzing Table IV and V, it is noticed that the implemented QSMF produced the best performance compared

to the existing switching filters in terms of the objective measures. It achieved a significantly larger value of PSNR under different types and density of noise for all the test images used. In addition, QSMF is able to achieve the best trade-off between noise suppression and image details preservation.

It can further be noted that the QSMF, QCDMF and HFC achieved the better performance than the other best performance proposed switching filters especially when filtering images corrupted with high noise density for the two noise models (p=0.3 for S&P and p=0.3 for RVI). The results also show that as the corruption level rises the QSMF outperforms the QCDMF and HFC for all the noise models in terms of PSNR.

V.IV. Visual Comparison

In this section, a visual comparison is employed to further analyse and verify the performance of the proposed filter. The filters selected for the visual comparison are the identity filter (IF) [11], the classical VMF [11], the QCDMF, the Adaptive Marginal Median Filter (AMMF) [16], the FAPGF, the HFC, the FTF, and finally the QSVMF-CLRD [28]. The 256×256 8-bit colour *Lena* and *Parrots* image were contaminated with 20% of S&P and RVI noise models respectively. The images are then restored using the listed methods, the comparison results are depicted in Fig. 9 and 10.

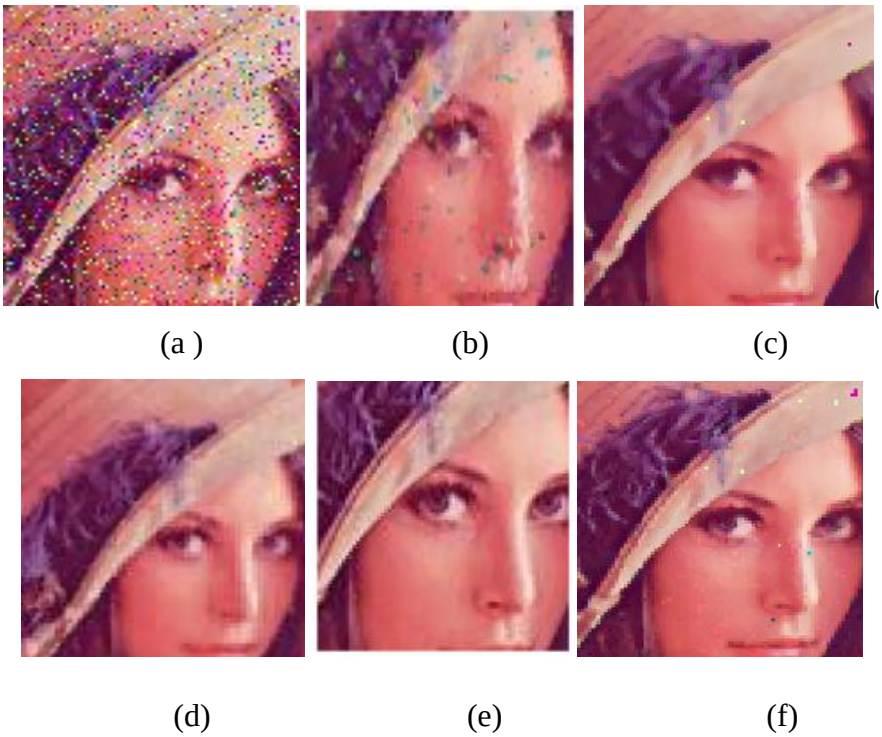

(a) (b) (c)

(d) (e) (f)

Fig. 9: Visual comparison using colour Lena image (a) Lena image contaminated by 20% of S&P noise (b) Output of AMMF (c) Output of VMF (d) Output of QCDMF (e) Output of HFC and (f) Output of QSMF (proposed)

Fig. 9 and 10 shows enlarged part of the test image *Lena* and *Parrots* filtered using the proposed QSMF and other classical switching methods. It can be seen that the VMF and HFC are superior to QSMF in terms of noise suppression capability. However, they over smoothed the image and thus results in distortion and loss of image fine details. Therefore, it can be deduced that the VMF and HFC filters slightly outperforms the proposed QSMF filter in terms of noise removal capability. However, the QSMF produced superior perceptual error performance and image details preservation capability, especially when the colour image is corrupted by high density impulse noise.

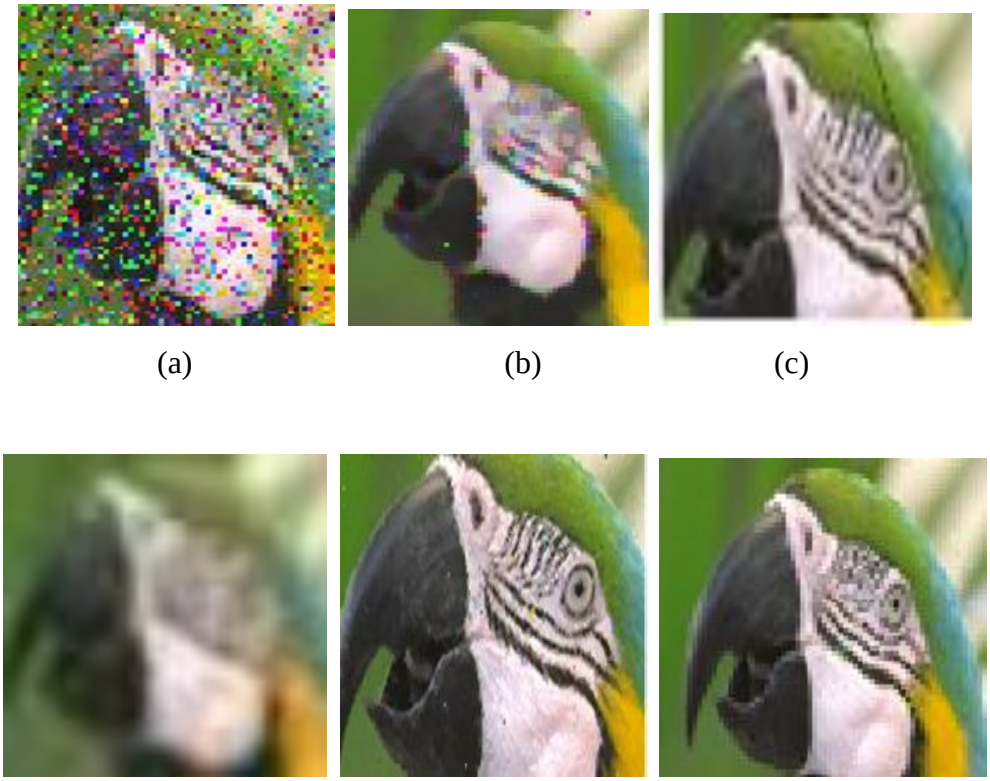

(a) (b) (c)

(d) (e) (f)

Fig. 10: Visual comparison using colour Parrot image (a) colour Parrot image contaminated by 20% of RVI noise (b) Output of VMF (c) Output of FAPGF (d) Output FTF (e) Output of QSVMF-CLRD and (f) Output of QSMF (proposed)

Thus, a general conclusion can be made that the proposed QSMF achieves an acceptable balance between the details preservation and noise suppression than the existing switching methods. It also produces the best filtering results in each case.

Note: similar results are obained using the remaining test images for all the experimets presented in this paper.

VI. CONCLUSION

In this paper, a new switching filter for suppression of impulse noise in colour images is introduced. The filter is based on the Quaternion transform theory and utilized the chromaticity differences, the intensity differences and the saturation differences between the colour pixels for detecting the corrupted pixels in an image. A vector median filtering process is employed to restore the contaminated pixels. With the use of quaternion theory, the three colour channels are processed simultaneously and thus achieved higher filtering efficiency. Experiments performed on test image set contaminated by two kinds of impulse noise model show that the proposed filter achieved an excellent results in terms of the four performance measures used. Based on the results presented and analyzed, the proposed filter achieves an acceptable balance between the image details preservation and noise suppression.

ACKNOWLEDGEMENTS

The authors want to express gratitude toward African Union (AU) for sponsoring this work.

REFERENCES

[1] Z. Gong, Z. Shen and K. Toh, Image Restoration with Mixed or Unknown Noises, *Multiscale Modeling & Simulation*, vol. 12, no. 2, April 2014, pp. 458-487.

[2] C. Lien, C. Huang, P. Chen, and Y. Lin, An Efficient Denoising Architecture for Removal of Impulse Noise in Images, *The IEEE Computer Society, vol. 62, no. 4*, December 2013, pp. 631–643.

[3] L. Jin, H. Liu, X. Xu, and E. Song, Quaternion-Based Impulse Noise Removal from Colour Video Sequence, *IEEE Transaction on Circuits and Systems for Video Technology, vol. 23, no. 5*, May 2013, pp. 741–755.

[4] Bhushan J, Ravishankar and Anitha HT, Impulse Noise Suppression Techniques in Digital Images : A Review, *International journal of Engineering Research Management and Technology, vol. 9359, no. 5*, May 2016, pp. 337–340.

[5] S. Dash, M. Bhaskar, B. Panigrahi and S. Das, *Artificial intelligence and evolutionary computations in engineering systems* (New Delhi: Springer, New Delhi, 2015).

[6] H. Ibrahim, K. C. Neo, S. H. Teoh, T. F. Ng, D. Chan, and J. Chieh, Impulse Noise Model and Its Variations, *International Journal of Computer and*

Electrical Engineering, v*ol. 4, no. 5*, October 2017, pp. 647–650.

[7] A. Rani and P. Gupta, High Density Impulse Noise Removal A Review, *International Journal for Research in Applied Science and Engineering, vol. 5, no. I,* January 2017, pp. 1613–1616.

[8] T. Mélange, M. Nachtegael, S. Schulte, and E. E. Kerre, A Fuzzy Filter for the Removal of Random Impulse Noise in Colour Video, *IEEE International Conference on Fuzzy System* ~ IEEE 2010~, *vol. 29, no. 6,* August 2010, pp. 407–419.

[9] J. Zhang and X. Tang, An Algorithm for Impulsive Noise Removal in Colour images, *Atlantis Press*, 2013, pp. 1513–1520.

[10] T. Mélange, M. Nachtegael, and E. E. Kerre, "Fuzzy Random Impulse Noise Removal from colour Image Sequences,"*IEEE Transaction on Image Processing, vol. 20, no. 4*, April 2011, pp. 959–970.

[11] X. Geng, X. Hu, and J. Xiao, Quaternion Switching Filter for Impulse Noise Reduction in Colour Image, *Elsevier Signal Processing, vol. 92, no. 1*, July 2012, pp. 150–162.

[12] M. E Celebi, H. A Kingravi and Y. A Asladogan, Nonlinear Vector Median Filtering for Impulsive Noise Removal from Colour Images, *Journal of Electronic Imaging,* v*ol. 16, no. 3,* 2007, pp. 1–65.

[13] A. Toprak, Impulse Noise Reduction in Medical Images with the use of Switch Mode Fuzzy Adaptive Median Filter, *Elsevier, Digital Signal Processing, vol. 17*, December, 2007, pp. 711–723.

[14] Z. Hosseinkhani, M. Hajabdollahi, N. Karimi, S. M. R. Soroushmehr, and S. Shirani, Adaptive Real - Time Removal of Impulse Noise in Medical Images, *Iran Michigan Centre for Integrative Research in Critical Care, University of Michigan USA*, 2016.

[15] M. V Sarode, Image Sequence Denoising with Motion Estimation in Color Image Sequences, *Engineering Technology and Applied Science Research, vol. 1,* 2011, pp. 139–143.

[16] S. Morillas and A. Sapena, Adaptive Marginal Median Filter for Colour Images, *Sensors Open Access Journal, March* 2011, pp. 3205–3213.

[17] B. Smolka, K. Malik, and D. Malik, Adaptive Rank Weighted Switching Filter for Impulsive Noise Removal in Colour Images, *Journal of Real-Time Image Processing,* December 2012, pp. 289–311.

[18] L. Malinski and B. Smolka, Fast Averaging Peer Group Filter for the Impulsive Noise Removal in colour Images, *Journal of Real-Time Image Processing*, May 2015.

[19] H. Hosseini, F. Hessar, S. Member, F. Marvasti, and S. Member, Real-Time Impulse Noise Suppression from Images Using an Efficient Weighted-Average

Filtering, *Sharif University of Technology*,Tehran Iran, August 2014, pp.1-11.

[20] Y. Dong, R. H. Chan, and S. Xu, A Detection Statistic for Random-Valued Impulse Noise Removal, *School of Mathematical Sciences, Peking University, Beijing China*, unpublished, *pp*. 1-17.

[21] Y. Dong and R. H. Chan, A New Detection Statistic for Random-Valued Impulse Noise Removal, *Mathematical Model for Multi-Channel Image Processing (MultIm'2006)*, 2006, pp. 1–4.

[22] S. Schulte, V. De Witte, M. Nachtegael, D. Van Der Weken, and E. E. Kerre, "Fuzzy Two-Step Filter for Impulse Noise Reduction From Colour Images," *IEEE Transactions on Image Processing, vol. 15, no. 11*, November 2006, pp. 3568–3579.

[23] S. K. Mishra, S. R. Chowdhury, and D. Mishra, A Fuzzy Impulse Noise Detection in Color Image," *Global Journal of Engineering, Science and Researches vol. 1, no. 5*, July 2014, pp. 5–8.

[24] D. Witte, M. Nachtegael, S. Schulte, D. Van Der Weken, and E. E. Kerre, Histogram-Based Fuzzy Colour Filter for Image Restoration, *Elsevier Image and Vision Computing, vol. 25,* 2007, pp. 1377–1390.

[25] J. Wang, and W. Liu, "Histogram-Based Fuzzy Filter for Image Restoration," *IEEE Transactions on Systems, Man and Cybernatics-Part B: Cybernetics, vol. 32, no. 2*, April 2002, pp. 230–238.

[26] G. Wang, Y. Liu, and T. Zhao, A Quaternion-Based Switching Filter for Colour Image Denoising, *Elsevie*r *Signal Processing, vol. 102,* March 2014, pp. 216–225.

[27] L. Chen, Y. Zhou, and C. L. P. Chen, "Quaternion-Based Colour Difference Measure for Removing Impulse Noise in Colour Images," *2014 International Conference on Informative and Cybernetics for Computational Social Systems ~ICCSS 2014~, no.5*, 2014, pp. 123–127.

[28] Z. Zhu, L. Jin, E. Song, and C. Hung, Quaternion Switching Vector Median Filter Based on Local Reachability Density, *IEEE Signal Processing*, *vol. 25, no. 6*, 2018, no. c, pp. 1–5.

[29] Z. Wang, A. C. Bovik, H. R. Shaikh and E. P. Simonceili, Image Quality Assesment: From Error Visibility to Structural Similarity, IEE Transaction on Image Processing, vol. 13, no. 4, April 2004, pp. 600-612

[30] J. Harikiran, B. Saichandana, and B. Divakar, Impulse Noise Removal in Digital Images, *International Journal of Computer Applications*, *vol. 10*, *no. 8*, November 2010, pp. 39–42.